Genetic differences between fibroelastic deficiency and Barlow's disease in mitral valve prolapse

Nina Feirer[1], Melanie Weber[1], Stefanie A Doppler[1], Katharina Knoll[2,3], Ling Li[2,3], Lucas Miranda[4], Mengyao Yu[5], Harald Lahm[1], Ehsan Vafadarnejad[1], Muamer Kameric[1], Tatjana Luzius[1], Sabine Seeler[1], Irina Gottmann[1], Felix Wirth[1], Marius Schwab[2,3], Arnar Geirsson[6], Peter Lichtner[7,8]; Aeron M Small[9,10,11]; Klaus Berger[12]; Monika Stoll[13]; Rüdiger Lange[1,3]; Peter Gruber[14]; Heribert Schunkert[2,3], Albert Hagége[15,16]; Nabila Bouatia-Naji[16]; Bertram Müller-Myhsok[17,18,19]; Teresa Trenkwalder[2,3]*; Markus Krane[1,3]*, Martina Dreßen[1]#*

(1) Department of Cardiovascular Surgery, Institute INSURE, TUM University Hospital German Heart Center, TUM School of Medicine and Health, Technical University of Munich (TUM), Germany

(2) Department of Cardiology, TUM University Hospital German Heart Center, TUM School of Medicine and Health, Technical University of Munich (TUM), Germany

(3) DZHK (German Center for Cardiovascular Research), Partner Site Munich Heart Alliance, Munich, Germany

(4) Max Planck Institute of Biochemistry, Munich, Germany

(5) Human Phenome Institute, Shanghai Pudong Hospital, Fudan University, Shanghai, China

(6) Department of Surgery, Section of Cardiac Surgery, Columbia University, New York, United States of America.

(7) Core Facility Genomics, Helmholtz Center Munich, Munich, Germany

(8) German Research Center for Environmental Health, Neuherberg, Germany

(9) Division of Cardiovascular Medicine, Brigham and Women's Hospital, Boston, Massachusetts.

(10) Center for Genomic Medicine and Cardiovascular Research Center, Massachusetts General Hospital, Boston, Massachusetts

(11) Program in Medical and Population Genetics and the Cardiovascular Disease Initiative, Broad Institute of MIT and Harvard, Cambridge

(12) Institute of Epidemiology & Social Medicine, University of Münster, Münster, Germany

(13) Department of Genetic Epidemiology, Institute of Human Genetics, University of Münster, Münster, Germany and Department of Biochemistry, Genetic Epidemiology and Statistical Genetics, Maastricht University, Maastricht, Netherlands

(14) Division of Cardiac Surgery, Yale University School of Medicine, New Haven, CT, USA

(15) AP-HP, Assistance Publique-Hôpitaux de Paris, Hôpital Européen Georges Pompidou, Department of Cardiology, Paris, France

(16) University of Paris Cité, Paris Cardiovascular Research Center (PARCC), Inserm, Paris, France

(17) Department of Translational Research in Psychiatry, Max Planck Institute of Psychiatry Munich, Munich, Germany

(18) HMNC Brainhealth, Munich, Germany

(19) Department of Health Data Science, University of Liverpool, Liverpool, United Kingdom

* senior authors contributed equally.

© The Author(s) 2026. Published by Oxford University Press on behalf of the European Society of Cardiology. This is an Open Access article distributed under the terms of the Creative Commons Attribution License (https://creativecommons.org/licenses/by/4.0/), which permits unrestricted reuse, distribution, and reproduction in any medium, provided the original work is properly cited.

ACCEPTED MANUSCRIPT

Downloaded from academic.oup.com/cardiovascres/advance-article/doi/10.1093/cvr/cvag263/9004318 by guest on 03 November 2026

This work was performed at the TUM University Hospital German Heart Center.

Corresponding author:

Dr Martina Dreßen

dressen@dhm.mhn.de

Department of Cardiovascular Surgery

TUM University Hospital German Heart Center

TUM School of Medicine and Health

Technical University Munich

Lazarettstrasse 36

Munich 80636

Germany

Tel: +49-89-1218-0

word count: 9,196/9,000 (main text plus title, abstract, legends, and references)

short title: FED versus Barlow's Disease in GWAS

Abstract

Aims

Fibroelastic deficiency (FED) and Barlow's disease represent subtypes of degenerative mitral valve prolapse (MVP). Whether these two conditions represent opposite ends of an anatomic spectrum or rather distinct etiologies remains unclear.

Methods and Results

To study this question from a genetic perspective, we conducted the first genome-wide association study (GWAS) on anatomical subtypes of MVP, exploring the MVP-Munich and

ACCEPTED MANUSCRIPT

Downloaded from academic.oup.com/cardiovascres/advance-article/doi/10.1093/cvr/cvag263/9004318 by guest on 03 November 2026

MVP-France cohorts, including 1,064 FED and 821 Barlow's disease cases, and 11,923 controls. Patients were stratified via echocardiographic and surgical reports. GWAS meta-analysis was performed separately for FED and Barlow's disease. The identified risk loci were analyzed via gene set enrichment analysis (GSEA), targeted variant-phenotype association analysis, and mitral valve tissue was analyzed in single-nucleus RNA-sequencing.

For FED, one risk locus achieved genome-wide significance (p<5e-8) at 5q23.3 (*CHSY3*). For Barlow's disease, two independent loci with genome-wide significance were identified at 5q35.2 (*CPLX2*) and 10q26.12 (*WDR11*). Further 30 additional independent signals showed a suggestive association (p<5e-5) with FED, and 30 different independent signals with Barlow's disease. Targeted variant-phenotype association analysis revealed an association of FED with atrial arrhythmias, while Barlow's disease was associated with atrial and ventricular arrhythmias. In combination with GSEA, our results linked Barlow's disease to changes in cell cycle, transcription, senescence, and ubiquitination. FED was connected to cardiac, valvular, mesoderm, and endoderm development.

Conclusions

This study suggests genetic heterogeneity between FED and Barlow's disease and identifies risk loci for future investigation.

ACCEPTED MANUSCRIPT

Downloaded from academic.oup.com/cardiovascres/advance-article/doi/10.1093/cvr/cvag263/9004318 by guest on 03 November 2026

Translational Perspective

This study marks an advance in the understanding of MVP by identifying the first genome-wide risk loci specific to FED and Barlow's disease. Our findings suggest that genetic differences between the two phenotypes may exist and support the need to separately investigate these two phenotypes. The identified loci highlight biological pathways that warrant further functional characterization and validation in independent cohorts. Improved understanding of subtype-specific genetic mechanisms may contribute to refining MVP classification, and to more precise risk stratification. Further research will be essential to confirm these findings and translate subtype-specific genetic insights into clinical practice.

Keywords

Mitral Valve Prolapse, Fibroelastic Deficiency, Barlow's Disease, GWAS, Meta-Analysis

Conference Abstracts

Genome-Wide Association Study in 2,140 Patients and Subtype Meta-analyses of Barlow's Disease and Fibroelastic Deficiency Identify Novel Risk Loci for Mitral Valve Prolapse

Thorac Cardiovasc Surg 2024; 72(S 01): S1-S68, DOI: 10.1055/s-0044-1780571

Highlighting Genetic Differences between Barlow's Disease and Fibroelastic Deficiency via Genome-Wide Association Study Meta-Analyses

ACCEPTED MANUSCRIPT

Downloaded from academic.oup.com/cardiovascres/advance-article/doi/10.1093/cvr/cvag263/9004318 by guest on 03 November 2026

Thorac Cardiovasc Surg 2025; 73(S 01): S1-S71, DOI: 10.1055/s-0045-1804116

Graphical Abstract

Key Question
Fibroelastic deficiency (FED) and Barlow's disease represent subtypes of degenerative mitral valve prolapse (MVP). Do these two conditions represent opposite ends of an anatomic spectrum or rather distinct disease etiologies?

Key Finding
Different risk loci with genome-wide significance on chromosome 5 and 10 were identified for FED and Barlow's disease in meta-analyses of the MVP-Munich and MVP-France cohort, including 1,064 FED and 821 Barlow's disease cases.

Take-home Message
This study suggests genetic differences between FED and Barlow's disease, emphasizing their distinct etiologies, providing a foundation for subtype-specific diagnostic markers and future therapeutic targets.

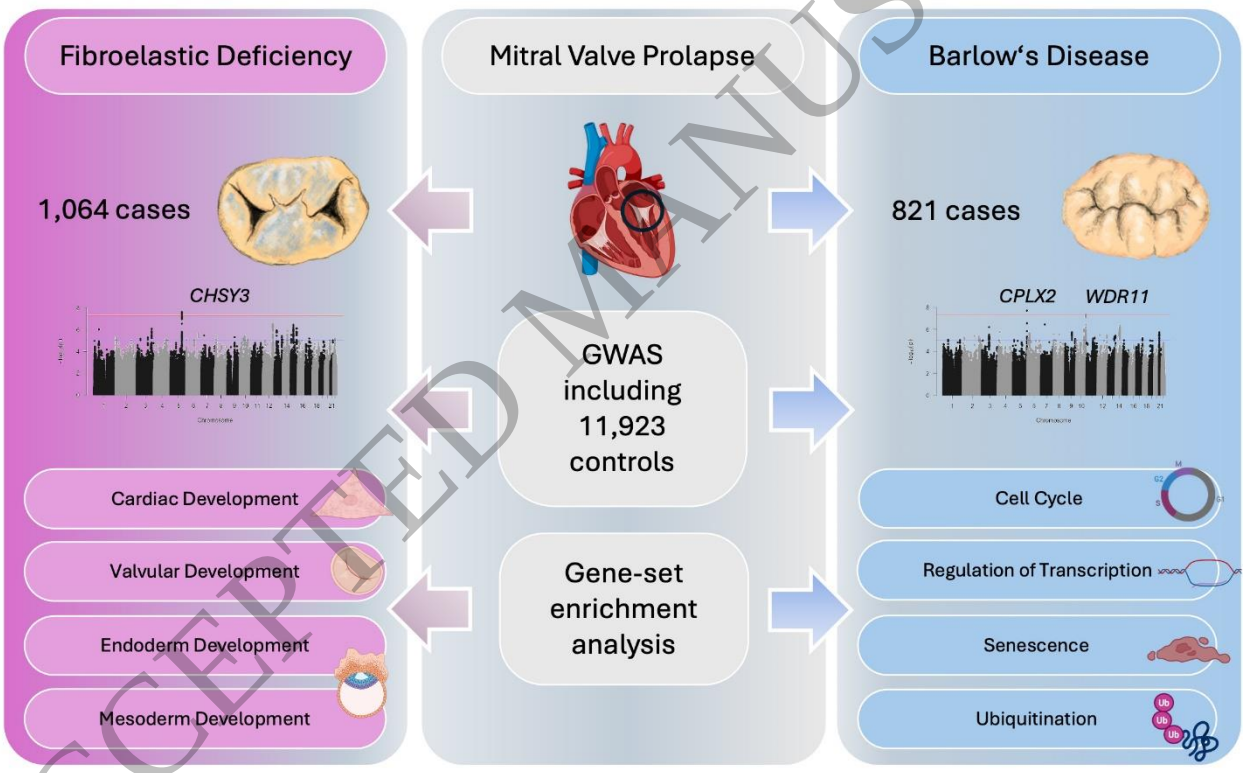


Figure Legend structured graphical abstract: Genetic Differences of Mitral Valve Prolapse Subtypes Fibroelastic Deficiency and Barlow's Disease. *CHSY3* = Chondroitin Sulfate Synthase 3, *CPLX2* = Complexin 2, GSEA = gene-set enrichment analysis, GWAS = genome-wide association study, *WDR11* = WD Repeat Domain 11; graphical elements partly created in https://BioRender.com

ACCEPTED MANUSCRIPT

Downloaded from academic.oup.com/cardiovascres/advance-article/doi/10.1093/cvr/cvag263/9004318 by guest on 03 November 2026

Abbreviations

DNA	Deoxyribonucleic acid
ECM	Extracellular matrix
FED	Fibroelastic Deficiency
GWAS	Genome-wide association study
ICD-10	International Statistical Classification of Diseases and Related Health Problems
MAF	Minor allele frequency
MPs	Macrophages
MR	Mitral regurgitation
MVP	Mitral valve prolapse
RNA	Ribonucleic acid
snRNAseq	Single-nucleus RNA sequencing
SE	Standard error
SNP	Single nucleotide polymorphism

ACCEPTED MANUSCRIPT

Downloaded from academic.oup.com/cardiovascres/advance-article/doi/10.1093/cvr/cvag263/9004318 by guest on 03 November 2026

1	UMAP	Uniform Manifold Approximation and Projection
2	VECs	Valvular endothelial cells
3	VICs	Valvular interstitial cells
4		
5		
6		

ACCEPTED MANUSCRIPT

Downloaded from academic.oup.com/cardiovascres/advance-article/doi/10.1093/cvr/cvag263/9004318 by guest on 03 November 2026

1. Introduction

Mitral valve prolapse (MVP), affecting 2-3% of the global population [1], is defined as a systolic mitral leaflet displacement towards the left atrium. [2] MVP can lead to mitral regurgitation, heart failure, and an increased risk of sudden cardiac death. [3,4] Symptomatic patients with severe MVP and patients with asymptomatic MVP combined with left ventricular dysfunction require cardiac surgery or valvular intervention. [3,4] Currently, there is no medical therapy for MVP. While syndromic forms of MVP have been identified, further research needs to elucidate the complex genetic architecture of non-syndromic forms of MVP. [5]

A genome-wide association study (GWAS) by Dina et al. identified risk loci associated with MVP, including *LMCD1, SIPA1L1* and *TNS1*, underlining the involvement of extracellular matrix (ECM) remodelling pathways in the pathogenesis of MVP. [6] Roselli et al. conducted a GWAS meta-analysis including six MVP datasets, identifying novel risk loci, including *SPTBN1, LTBP2, TGFB2, NMB, and ALPK*. Additionally, the group developed a new polygenic risk score to improve MVP susceptibility prediction. [7]

The broad spectrum of degenerative MVP includes two distinct subtypes: fibroelastic deficiency (FED) and Barlow's disease, characterized by unique pathological mechanisms as well as striking differences in clinical presentation. Barlow's disease has been more strongly linked to heritable and polygenic mechanisms, whereas FED has traditionally been considered more degenerative and age-related. However, occurrence in younger patients and familial clustering suggest that genetic factors may also contribute to

ACCEPTED MANUSCRIPT

Downloaded from academic.oup.com/cardiovascres/advance-article/doi/10.1093/cvr/cvag263/9004318 by guest on 03 November 2026

FED.[6,8–10] FED is associated with localized thinning and fibroelastic tissue loss, often affecting older patients. [10,11] Conversely, Barlow's disease is characterized by diffuse myxomatous degeneration with thickened and enlarged leaflets, occurring frequently in younger patients. [10,11]

Genetic differences between the two MVP subtypes have not yet been investigated. This study focuses on advanced MVP, as our cohort includes predominantly patients requiring surgery. We aimed to perform the first GWAS analyses of FED and Barlow's disease using two cohorts of precisely phenotyped MVP cases analyzing their distinct genetic compositions.

2. Results

2.1 Mitral valve prolapse study population

A total of 1,825 patients undergoing cardiac surgery for degenerative MVP from the Department of Cardiovascular Surgery were identified. Sixteen patients with insufficient information for classification (n=14: MVP, n=2: only tendon tear) were excluded from the analysis, resulting in 1,809 patients (n=1,251 male, n=558 female) included in the study. Of these surgical patients, a subset of 87 patients had a history of previous cardiac surgery, including prior mitral valve surgery. Furthermore, 331 (n=219 male, n=112 female) patients with symptomatic MVP were included from the Department of Cardiology. Of the

ACCEPTED MANUSCRIPT

Downloaded from academic.oup.com/cardiovascres/advance-article/doi/10.1093/cvr/cvag263/9004318 by guest on 03 November 2026

cardiological patients, 82 had previous mitral valve surgery for degenerative MVP and were followed in the outpatient setting.

After imputation and quality control, 2,039 patients (95.3%) remained for further analyses. Additionally, 9,484 controls from the PROCAM-2 cohort were included in the analyses. [12,13]

Stratification of the MVP-Munich cohort into subgroups revealed 953 FED and 402 Barlow's disease cases. In 785 cases, a clear stratification into FED or Barlow's disease was not possible, so these patients were defined as "intermediate" cases and excluded from further analyses. Of the FED and Barlow's disease patients (cardiology and cardiac surgery), 85 patients (6.3%) had previous mitral valve surgery. Baseline patient characteristics are detailed in *Supplementary Table 1*. Patients with Barlow's disease were significantly younger than FED patients (56.9 years (±13.4) vs. 65.8 years (±12.1), p<0.001) and had fewer comorbidities.

For meta-analysis, we included participants from the MVP-France study [6], where MVP disease phenotypes were available and included 111 FED and 419 Barlow's disease cases, as well as 2,439 controls. Fig. 1 gives an overview of the GWAS meta-analyses, consisting of the MVP-Munich and the MVP-France cohort, which in total included 1,064 cases of FED, and 821 cases of Barlow's disease, respectively.

[Fig. 1]

ACCEPTED MANUSCRIPT

Downloaded from academic.oup.com/cardiovascres/advance-article/doi/10.1093/cvr/cvag263/9004318 by guest on 03 November 2026

2.2 GWAS Meta-Analyses

For subgroup meta-analyses, global inflation factor was λ = 1.1 for FED, and λ = 1.1 for Barlow's disease. The corresponding Manhattan Plots are depicted in Fig. 2 and 3. Quantile-Quantile plots can be found in the *Supplementary Fig. 1*.

GWAS meta-analysis for FED identified a single risk locus with genome-wide significance ($p<5x10^{-8}$) on chromosome 5q23.3 (Table 1). The regional plot is depicted in Fig. 4A. The independent lead SNP is *rs2108427_T* (β = 0.267, SE = 0.058), the nearest gene is Chondroitin Sulfate Synthase 3 (*CHSY3*). There were an additional 30 suggestive loci ($p<5x10^{-5}$) for FED. Lead SNPs for each suggestive locus are listed in *Supplementary Table 3*. SNPs with very strong effect sizes were: rs77907459_T (β = -0.699, SE = 0.155, nearest gene: *PERP*), and rs59300919_A (β = 0.471, SE = 0.122, nearest gene: *WDR93*).

GWAS meta-analysis for Barlow's disease revealed two genome-wide significant independent loci associated with the disease on chromosome 5q35.2 (*rs4868539_A*) and 10q26.12 (*rs7920943_A*), respectively (Table 1). Regional plots are depicted in Fig. 4. The lead SNP *rs4868539_A* demonstrated an effect size of β = -0.336386 (SE = 0.0850879), the nearest gene is Complexin 2 (*CPLX2*). The lead SNP *rs7920943_A* demonstrated an effect size of β = 0.438517 (SE = 0.0889497), and WD Repeat Domain 11 (*WDR11*) was identified as the nearest gene. An additional 30 suggestive loci were identified in Barlow's disease meta-analysis and are listed in *Supplementary Table 4*. SNPs with very strong effect sizes were: rs35010130_G (β = -0.520, SE = 0.153, nearest gene: *FBXL7*), *rs56360275_G* (β =

ACCEPTED MANUSCRIPT

Downloaded from academic.oup.com/cardiovascres/advance-article/doi/10.1093/cvr/cvag263/9004318 by guest on 03 November 2026

0.523, SE = 0.123, nearest gene: *POU1F1*), *rs139982410_T* (β = 0.593, SE = 0.139, nearest gene: *TAOK3/PEBP1*), and *rs71448926_C* (β = 0.594, SE = 0.138, nearest gene: *RDH14*).

The genome-wide significant signal for FED was not found as significant signal in the Barlow's disease meta-analysis, and vice versa (Fig. 4). The same applies to the suggestive signals – neither were found as significant signals in the respective other entity.

[Fig. 2,3,4, Table 1]

2.3 Gene set enrichment analysis

GSEA of the 53 FED associated genes revealed an enrichment in developmental processes (Fig. 5A), specifically mesoderm and endoderm development as well as cardiac development (*Supplementary Table 5*). Furthermore, gene sets for cardiac valve development and cardiac diseases showed a strong enrichment (Fig. 5A).

In GSEA performed for Barlow's disease, 55 associated genes were included. Most associations were found for the following categories: regulation of transcription, cell cycle, ubiquitination, and senescence (Fig. 5B).

[Fig. 5]

2.4 Targeted variant-phenotype association analysis

Targeted variant-phenotype association analysis between suggestive loci ($p<e-5$) associated with FED or Barlow's disease and MVP-related traits identified ten significant associations ($p<0.05$). The five respective lead SNPs for FED or Barlow's disease and

ACCEPTED MANUSCRIPT

Downloaded from academic.oup.com/cardiovascres/advance-article/doi/10.1093/cvr/cvag263/9004318 by guest on 03 November 2026

related phenotypes are depicted in Fig. 6. Further loci are detailed in *Supplementary Table 6* and *Supplementary Fig. 2*.

For Barlow's disease, four suggestive loci were associated with cardiac traits. The lead SNP *rs11195347_T* is associated with atrial fibrillation and left ventricular hypertrophy, also, *rs56360275_G* and showed an association with left ventricular hypertrophy. *rs960391_T* was associated with left ventricular hypertrophy, ventricular arrhythmia, and paroxysmal supraventricular tachycardia. *rs72826619_C* is associated with a reduced risk of ventricular arrhythmia. One lead SNP of FED, *rs10024673_T*, was associated with atrial fibrillation and paroxysmal supraventricular tachycardia.

[Fig. 6]

2.5 Single-nucleus RNA sequencing

Single-nucleus RNA sequencing (snRNAseq) of mitral valve tissue yielded 11,435 nuclei for downstream analysis after quality control. Uniform Manifold Approximation and Projection (UMAP) visualization revealed distinct cellular clusters, including valvular interstitial cells (VICs), valvular endothelial cells (VECs), macrophages (MPs), lymphoid cells, a melanocyte-like cluster and a myofibroblast cluster (Fig. 7A). Canonical marker genes used to define the clusters are shown in Fig. 7B. Heatmaps illustrate the cell-type specific expression of the prioritized genes, *CHSY3* for FED, and *CPLX2* and *WDR11* for Barlow's disease and genes associated with FED or Barlow's disease that are overrepresented in pathways identified by GSEA (Fig. 5) in the adult mitral valve (Fig. 7C, D). The snRNAseq reference dataset was used to identify the mitral valve

ACCEPTED MANUSCRIPT

Downloaded from academic.oup.com/cardiovascres/advance-article/doi/10.1093/cvr/cvag263/9004318 by guest on 03 November 2026

cell populations expressing GWAS-prioritized genes and to provide cell-type specific biological context for the associated loci.

[Fig. 7]

3. Discussion

This study represents the first GWAS focusing on subtypes of degenerative MVP. Meta-analyses included 1,064 cases of FED and 821 cases of Barlow's disease. For FED, a risk locus with genome-wide significance was identified on chromosome 5q23.3 (*CHSY3*). GWAS meta-analysis for Barlow's disease yielded two independent loci with genome-wide significant associations on chromosome 5q35.2 (*CPLX2*) and 10q26.12 (*WDR11*). Genetic signals found for FED did not appear in the entity of Barlow's disease, and vice versa (Fig. 4).

Our data support the hypothesis that FED and Barlow's disease could represent different genetic entities. Barlow's disease typically presents in younger patients with pronounced myxomatous degeneration of the mitral valve, characterized by bileaflet thickening, enlargement, and extensive mitral annular disjunction. [10,11] More common in older individuals, FED is associated with a paucity of connective tissue, leading to chordal rupture and isolated mitral valve leaflet prolapse without significant annular disjunction. [14] Accordingly, Barlow's patients in the MVP-Munich cohort were younger and had fewer pre-existing conditions than FED patients. [15]

ACCEPTED MANUSCRIPT

Downloaded from academic.oup.com/cardiovascres/advance-article/doi/10.1093/cvr/cvag263/9004318 by guest on 03 November 2026

Interestingly, the only suggested association in both FED and Barlow's disease was found for a locus near *SIPA1L1* (14q24.2). Accordingly, an association of *SIPA1L1* with degenerative MVP has been implicated previously. [6] Although *SIPA1L1* is known to be expressed in neurons and involved in synaptic activity [16], we found the transcript in MPs in snRNAseq of mitral valve tissue.

Furthermore, *RBM20* and *MEOX1* were described as MVP candidate genes by Roselli et al. [7] In our subgroup meta-analyses we observed a suggestive association of *MEOX1* with FED, and of *RBM20* with Barlow's disease. In the targeted variant-phenotype association analysis *RBM20* was also associated with left ventricular hypertrophy. Previous studies have linked *RBM20* mutations to dilatative cardiomyopathy, potentially compromising the integrity of cardiac valves. [17] *MEOX1*, a transcription factor involved in mesodermal development, can drive pathological remodeling via upregulation of *GATA4*, another transcription factor that we also found to be associated with FED. [18,19]

Our data revealed a suggested association of *SEPTIN9 (SEPT9)* specifically with Barlow's disease. Moore et al. demonstrated that a *DCHS1-LIX1L-SEPT9* axis promotes filamentous actin organization, directing cell-ECM alignment and thereby shaping valve tissue. [20] *DCHS1* has been linked to MVP without specific subtype stratification by Durst et al. [21] before, without assigning it to an MVP subtype.

A genome-wide significant association with FED was identified at a risk locus on Chromosome 5, with *CHSY3* (5q23.3) as the nearest gene. *CHSY3* is involved in the Chondroitin sulfate/dermatan sulfate and glycosaminoglycan metabolism. [22]

ACCEPTED MANUSCRIPT

Downloaded from academic.oup.com/cardiovascres/advance-article/doi/10.1093/cvr/cvag263/9004318 by guest on 03 November 2026

Glycosaminoglycans in fetal heart valves contribute to valve tissue maturation, [23] suggesting that *CHSY3* could indirectly influence ECM composition. SnRNAseq data from mitral valve tissue revealed *CHSY3* expression in VICs and myofibroblasts of the adult mitral valve, indicating a potential role for *CHSY3* also in mature mitral valves. Supporting this, another study found significantly increased levels of chondroitin/dermatan 6-sulfate and hyaluronan in affected mitral valve chordae. [24] Chordal rupture is a typical pathological finding in MVP, particularly in FED. Altered glycosaminoglycan content and distribution in degenerative mitral valve tissue are thought to reduce mechanical tension and disrupt matrix microstructure contributing to tissue weakening. [25] These findings may relate to the typical mechanical weaknesses and subsequent failing of leaflets and chordae in FED valves. [24,26]

An interesting candidate region with a strong effect size and suggested association with FED is near the gene *PERP* (6q23.3). *PERP* is localized in the plasma membrane, and its induction is linked to apoptosis in fibroblasts. [27] Fibroblasts, or VICs in valvular tissue, play a pivotal role in maintaining the mitral valve integrity by building and remodeling the ECM. [28,29] Disruption may lead to fibrosis and structural remodeling of the ECM, which are associated with the development and progress of MVP. [28,29] *COL4A2* (13q34), a structural component of the ECM [30], showed a suggested association with FED and was predominantly expressed in myofibroblasts. Changes in the ECM are key contributors in MVP development. [28,29] These findings implicate that *PERP* and *COL4A2* are involved in ECM remodeling and fibrosis, likely contributing to the FED phenotype. *COL4A2* was also found in enriched gene sets associated with endoderm and mesoderm development

ACCEPTED MANUSCRIPT

Downloaded from academic.oup.com/cardiovascres/advance-article/doi/10.1093/cvr/cvag263/9004318 by guest on 03 November 2026

processes. GSEA further revealed suggested enrichment for pathways related to cardiac and valve development (Fig. 5A). Enrichment was driven by transcription factors such as *GATA4* and *TBX20* (Fig. 5A, *Supplementary Table 5*), both of which are well-established regulators of heart development. [31] *GATA4* (8p23.1) showed a suggestive association with FED and is essential for the epithelial-to-mesenchymal transition (EMT) of atrioventricular valves. [32] Mutations in *GATA4* impair its interaction with *SMAD4*, resulting in atrioventricular septal defects and valve abnormalities. [33] *TBX20* (7p14.2) was mainly expressed in VICs of mitral valve tissue, which are initiators of collagen synthesis and degradation in valve leaflets. [34] *TBX20* may be involved in cardiac development by regulating the *Wnt* pathway to direct endocardial cushion maturation and valve elongation. [35] Notably, several transcription factors essential for development were also expressed in the adult mitral valve, primarily in VICs, VECs, and myofibroblasts (Fig. 7C). This suggests that these factors retain functional relevance in the adult valve. Our findings are in line with the notion that FED is a slowly progressing disease, necessitating mitral valve surgery in older patients compared to Barlow's disease.

Our genome-wide association identified *CPLX2* (5q35.2) and *WDR11* (10q26.12) as nearest genes for Barlow's disease. Three highly significant SNPs were detected near CPLX2. CPLX2 encodes a synaptic vesicle-associated protein with predominant expression in neuronal tissue and no established role in cardiac or valvular biology. [36–40] Given the linkage disequilibrium structure of this locus, the observed association signal may be driven by regulatory variation affecting CPLX2 or by another nearby gene. At present, no

ACCEPTED MANUSCRIPT

Downloaded from academic.oup.com/cardiovascres/advance-article/doi/10.1093/cvr/cvag263/9004318 by guest on 03 November 2026

mechanistic conclusions can be drawn, and the causal gene and biological relevance of this locus in mitral valve disease remain to be determined.

WDR11, which is involved in cell cycle progression, signal transduction, apoptosis, and gene regulation, has been proposed to function as a tumor suppressor gene. [41,42] In addition, *WDR11* has previously been implicated in Hedgehog and primary cilia signalling, and *WDR11*-null mice exhibit developmental cardiac defects.[9] Disruption of cilia-related pathways has been linked to familial mitral valve prolapse through variants in *DZIP1*, suggesting that altered ciliary signalling may represent a biologically plausible mechanism contributing to mitral valve prolapse.[9] GSEA of Barlow's disease associated genes also suggested a link to pathways relevant for regulation of cell cycle. Considering these functions, *WDR11* could contribute to the development of Barlow's disease, although further studies are necessary. *WDR11* also showed a significant association with ventricular arrhythmias in the targeted variant-phenotype association analysis. These observations provide additional support for the potential relevance of the *WDR11* locus identified in the present study, although further functional studies will be required to establish causality.

FBXL7 is the nearest gene to a candidate region with a strong effect size and suggested association with Barlow's disease. *FBXL7* targets *Aurora A* for polyubiquitylation, leading to mitotic cell cycle arrest. [43] It also mediates phosphorylation-dependent ubiquitination. [44] *USP35* (11q14.1), a gene near a candidate region with suggested association with Barlow's disease, regulates cell mitosis by deubiquitinating *Aurora B*. [45,46] *USP35* was expressed in VECs, indicating its involvement in the adult mitral valve. These

ACCEPTED MANUSCRIPT

Downloaded from academic.oup.com/cardiovascres/advance-article/doi/10.1093/cvr/cvag263/9004318 by guest on 03 November 2026

findings suggest that dysregulation of ubiquitination may influence the ECM remodeling, thereby contributing to the myxomatous phenotype of Barlow's disease. Interestingly, ubiquitination showed a suggested enrichment in GSEA. For the first time, genes involved in ubiquitination and deubiquitination, and key regulators of protein degradation were linked to the pathogenesis of Barlow's disease. In addition, GSEA of Barlow's disease associated genes showed a suggested link to pathways relevant for regulation of transcription and senescence (Fig. 5, 7C). H4C1, H4C2, and H3C1, are components of nucleosome wrapping, contributing to chromosomal stability. [47–49] By epigenetic modulation of ECM remodeling, these processes may contribute to the myxoid degeneration and leaflet thickening characteristic for Barlow's disease. The enrichment in senescence-associated terms (Fig. 5) might be associated with the "earlier onset" of Barlow's disease compared to FED.

While *COL4A2* was associated with FED, *COL4A1* showed a suggested association with Barlow's disease. As a member of the type IV collagen family, it functions as an ECM structural constituent. [30] **During the formation of the ECM, integrins are responsible for myocyte-to-collagen connections.** [50,51] Dysregulation of ***TGF-β*** signaling can induce ECM production in cultured VICs of myxomatous mitral valves. [52,53] Also, mTOR activation from abnormal integrin-dependent cell-matrix interactions can drive ***TGF-β*** overactivity and myxomatous mitral valve degeneration.[54] **Thus, integrin-mediated adhesion as well as the *TGF-β* pathway are important for maintaining the mechanical integrity of the mitral valve.**

ACCEPTED MANUSCRIPT

Downloaded from academic.oup.com/cardiovascres/advance-article/doi/10.1093/cvr/cvag263/9004318 by guest on 03 November 2026

Overall, disruptions in cell cycle regulation, apoptosis, and myxomatous degeneration can contribute to valvular degeneration. Genes such as *CPLX2*, *WDR11*, *FBXL7*, and *COL4A1* may play important roles in ECM-cell interactions and remodeling, either directly or via ubiquitination-dependent mechanisms. These processes may contribute to the myxoid degeneration and leaflet thickening characteristic for Barlow's disease.

A major strength of this study lies in its meta-analysis of precisely phenotyped cohorts to ensure robust statistical power and reliable detection of genetic associations. The clinical characterization of Barlow's disease and FED represents the first worldwide GWAS with precise stratification of MVP subtypes. We identified novel risk loci separately for FED and Barlow's disease.

For the first time, this study allowed an association of known and novel genes with the MVP subtypes FED and Barlow's disease. Additionally, we employed state-of-the-art analytical tools, including high-quality functional annotation, to refine associations and interpret their biological relevance. The comprehensive QC process, high-quality imputation, and use of population-matched LD reference panels are of notable strength. These measures minimized biases and ensured reliability of genetic associations.

However, some limitations remain when interpreting the findings of our study. The study was conducted in patients of European ancestry and 69.9% were male, potentially not covering all relevant genetic variants. The study's power to detect rare variants was constrained by the minor allele frequency (MAF) threshold of 0.01, eventually overlooking rare but impactful genetic contributions. We acknowledge that, given the modest sample

ACCEPTED MANUSCRIPT

Downloaded from academic.oup.com/cardiovascres/advance-article/doi/10.1093/cvr/cvag263/9004318 by guest on 03 November 2026

sizes of 1,064 FED and 821 Barlow's cases by contemporary GWAS standards, our study is primarily powered to detect common genetic variants with moderate to large effect sizes. As a consequence, some of the reported effect sizes may be inflated compared to those in larger independent replication cohorts and are expected to attenuate with increasing sample size. Furthermore, no independent replication cohort was available for validation of the observed associations. The identified loci should therefore be considered preliminary candidate regions that require confirmation in larger independent studies and further functional investigation before conclusions regarding subtype-specific genetic mechanisms can be drawn. While shrinkage-based effect estimation approaches could further address this issue, we have chosen to emphasize cautious interpretation of the reported effect sizes and the need for independent replication. Further, the study's power could be reduced by examining disease subgroups, thereby incorrectly yielding suggestive associations. Also, the patients included predominantly suffered from severe forms of MVP requiring surgery or intervention. The classification into subgroups was not assessed via formal inter-rater agreement. As echocardiographic data were not available in the control cohort, the presence of subclinical or undiagnosed MVP could not be excluded. Detailed individual-level information on cardiovascular risk factors and lifestyle characteristics was not uniformly available across all cohorts, precluding formal case-control comparisons and adjustment for these variables. GSEA pathway analyses are based on genes annotated to suggestive loci and should therefore be interpreted as hypothesis-generating. Functional validation and gene expression data from mitral valve tissue will be required to confirm these observations. Regarding the targeted variant-phenotype association analysis, the

ACCEPTED MANUSCRIPT

Downloaded from academic.oup.com/cardiovascres/advance-article/doi/10.1093/cvr/cvag263/9004318 by guest on 03 November 2026

cause of cardiac arrhythmia predominantly lies in the cardiac tissue, not per se in the valve tissue, and therefore other correlations might have been missed. Furthermore, our cohort consists predominantly of patients with advanced, surgically treated MVP, which may explain the discordant association of reduced risks in the targeted variant-phenotype association analysis for arrhythmias. The identified variants could reflect genetic drivers of valvular degeneration rather than atrial remodeling. The lack of association with MVP or MR likely reflects differences in phenotype definition, as subtype-specific genetic effects identified in our surgically characterized cohort may not be captured in heterogeneous ICD-based datasets.

Sex-stratified analyses would add valuable information to the already known sex differences in MVP presentation, however, our study is underpowered for such analyses. Future studies could provide valuable insights regarding possible differences regarding the subtypes FED and Barlow's disease. Additionally, while computational tools provided functional annotations, the lack of experimental validation leaves the biological mechanisms speculative, and therefore, further studies are required to validate the functional roles of the implicated genes. Importantly, the snRNAseq data were derived from a limited number of post-mortem control samples, and the absence of diseased MVP tissue (FED or Barlow's disease) for direct comparison represents a key limitation that should be addressed in future studies. In addition, the post-mortem interval ranged from two to three days, and therefore potential effects of agonal events or post-mortem tissue changes, particularly within immune cell populations, cannot be completely excluded.

ACCEPTED MANUSCRIPT

Downloaded from academic.oup.com/cardiovascres/advance-article/doi/10.1093/cvr/cvag263/9004318 by guest on 03 November 2026

Finally, there is currently no validation cohort available reflecting FED and Barlow's disease stratification.

The loci identified in this study hold substantial potential for risk stratification and early diagnosis of MVP. Understanding the genetic basis of Barlow's disease and FED could pave the way for personalized therapeutic strategies targeting subtype-specific pathways. In particular, pathways related to ECM remodeling emerge as interesting therapeutic targets. The integration of the detected risk loci into polygenic risk scores may further enhance individualized risk prediction, allowing earlier interventions for high-risk individuals. Nevertheless, translating these findings into clinical applications will require further studies, including functional investigations to clarify the biological relevance of the identified loci and independent replication in larger cohorts. Additional analyses focusing on specific mitral valve structures, such as the chordae tendineae, may provide further mechanistic insights into disease heterogeneity.

In conclusion, this study identifies genome-wide significant loci associated with fibroelastic deficiency and Barlow's disease and provides evidence for potential genetic differences between these mitral valve prolapse subtypes. These findings refine the current understanding of the genetic architecture of MVP and support the concept that FED and Barlow's disease may, at least in part, be driven by distinct genetic determinants. Further replication in independent cohorts and functional studies will be essential to confirm these observations and elucidate their biological relevance.

ACCEPTED MANUSCRIPT

Downloaded from academic.oup.com/cardiovascres/advance-article/doi/10.1093/cvr/cvag263/9004318 by guest on 03 November 2026

4. Methods

4.1 Patients and Controls

The MVP-Munich cohort includes patients of European descent that underwent mitral valve surgery at the Department of Cardiovascular Surgery or presented with MVP and mitral regurgitation (MR) at the Department of Cardiology at the TUM University Hospital German Heart Center between March 2002 and January 2021. The severity of MR was classified according to the current ESC/EACTS guidelines, see also *Supplementary Methods*. [55] The control cohort for MVP-Munich included European participants from the PROCAM-2 cohort. [12,13]

Exclusion criteria were mitral stenosis (moderate or severe), ischemic MR, endocarditis, and re-operation if the primary etiology of the defect was unknown. Also, patients suffering from MR associated with a syndrome (e.g., Marfan) or another cardiac disease (e.g., rheumatic disease) were excluded. Baseline clinical and surgical characteristics were collected from the internal clinical database of the TUM University Hospital German Heart Center. Surgical reports as well as echocardiographic data were used to differentiate between functional and degenerative MR. Detailed baseline characteristics are provided in *Supplementary Table 1*.

Mitral valve prolapse classification was in 90% of the surgical cases based on descriptions from direct inspection of the valve provided in the surgical report. If surgical reports lacked detail or in non-surgical cases, echocardiographic findings were reviewed. A

ACCEPTED MANUSCRIPT

Downloaded from academic.oup.com/cardiovascres/advance-article/doi/10.1093/cvr/cvag263/9004318 by guest on 03 November 2026

stratification into subgroups *FED – Intermediate – Barlow's disease* was performed. Cases were classified as FED when there was a simple prolapse of one leaflet or when the valve was described as "FED valve" in the surgical report. Slightly thickened leaflets were included in this category if the prolapse was isolated to a single leaflet.

Cases were classified as Barlow's disease based on explicit mention in the surgical report, doctor's letter, or echocardiographic findings. This classification was assigned to valves exhibiting prolapse of multiple leaflets and significant thickening, or if a "massive prolapse," particularly of multiple leaflets, was described.

The surgical report was used for classification in over 90% of cases. The remaining cases were defined by echocardiographic findings, which were guided by descriptions adapted from the visual framework by Levine et al.[2]

Valves that could not be distinctly classified as either FED or Barlow's disease were labeled as intermediate. These valves displayed some thickening but did not meet criteria for Barlow's disease. These cases were not included in the GWAS meta-analyses to ensure the sharpest possible distinction between the subgroups.

French patients were classified as Barlow disease or FED based on standardized echocardiographic evaluation and, when available, intraoperative findings from mitral valve surgery as reported previously.[6] In brief, echocardiographic recordings and operative reports were centrally reviewed to ensure consistent phenotyping across participating centers.

ACCEPTED MANUSCRIPT

Downloaded from academic.oup.com/cardiovascres/advance-article/doi/10.1093/cvr/cvag263/9004318 by guest on 03 November 2026

Meta-analyses were performed with datasets obtained in cooperation with the investigators of the MVP-France cohort. The MVP-France study (*Genetic polymorphisms in idiopathic mitral valve prolapse: A French prospective study*) is a prospective multicenter nation-wide study promoted by the French Society of Cardiology. [6,56] Controls were obtained from the MVP-France cohort as well. The German GWAS used controls exclusively from the PROCAM cohort, whereas the French GWAS used controls exclusively from the Three-City (3C) Study[57], with no overlap between the control populations. Patients from MVP-France were stratified by the MVP-France investigators into the subgroups by information from the surgical reports in the majority of cases. Details on the MVP-France cohort have been published previously by Dina et al. [6], see also the associated Supplementary for the study by Dina et al. (*Supplementary Table 1*). Detailed cardiovascular and lifestyle variables were unavailable for the French discovery cohort due to recruitment design.

4.2 DNA extraction, genotyping, and imputation

DNA extraction was performed using the QIAamp DNA Blood Mini Kit (QIAGEN, Hilden, Germany). For the isolation of genomic DNA, the buffy coat of blood samples was used. DNA quality was verified via gel electrophoresis. The concentration was determined using NanoDrop (ThermoFisher Scientific, Waltham, MA, USA).

Genotyping and quality control was performed at the *Helmholtz Center Munich* using the Infinium Global Screening Array (GSA MD V3 and Control Dashboard, Illumina, San Diego, CA, USA). Participants with genotype call rates <98% and individual

ACCEPTED MANUSCRIPT

Downloaded from academic.oup.com/cardiovascres/advance-article/doi/10.1093/cvr/cvag263/9004318 by guest on 03 November 2026

heterozygosity levels <10,000 were excluded. Single nucleotide polymorphisms (SNPs) with a minor allele frequency (MAF) <0.05 and a call rate <95% were excluded. SNPs with an exact Hardy-Weinberg equilibrium *P*-value of <0.0001 in controls and $<1\times10^{-7}$ in demographically homogenous cases were excluded. For large-scale imputation, the genotyped SNPs of cases and controls were pre-phased via the SHAPE-IT (v2) program. [58] The imputation of 4.8 million common SNPs (MAF <0.01 in 1000 Genomes Project Europeans, phase 3 haplotype reference panel), [59] was carried out using IMPUTE (v2) [60]. Standard post-imputation quality control was performed. SNPs were selected for linkage disequilibrium (LD) independence ($r^2 > 0.2$).

4.3 Genome-wide association analysis

GWAS was performed with the software PLINK (Version 1.9 and 2.0). [61] Linear regression was applied for continuous traits, while logistic regression was used for binary traits, with covariates including age, sex, and principal components (the first ten to account for population stratification). To adjust for population stratification, multidimensional scaling was performed in PLINK. [62] To account for population stratification, multidimensional scaling (MDS) analysis was performed using PLINK based on pairwise genetic distances. The first ten MDS components (C1–C10) were included as covariates in the logistic regression models.

4.4 French discovery cohort

The French discovery cohort consisted of 419 patients with Barlow disease (BD), 111 patients with fibroelastic deficiency (FED), and 1,562 controls from the Three-City (3C)

ACCEPTED MANUSCRIPT

Downloaded from academic.oup.com/cardiovascres/advance-article/doi/10.1093/cvr/cvag263/9004318 by guest on 03 November 2026

Study.[57] All participants were of European ancestry. MVP cases were clinically characterized using standardized echocardiographic assessment and/or surgical information. Genome-wide association analyses were performed using PLINK2 under an additive genetic model, adjusting for sex and the first five principal components (--covar-name sex,cov_1,cov_2,cov_3,cov_4,cov_5; --glm). Variants with minor allele count <5, minor allele frequency <0.01, or imputation quality (Mach R^2) <0.8 were excluded (--mac 5; --maf 0.01; --mach-r2-filter 0.8). Genotype imputation was performed using the 1000 Genomes Project reference panel.

4.5 Meta-analysis

Both MVP cohorts were stratified into FED and Barlow's disease subgroups. Subgroup GWASs were performed in PLINK 2.0. To combine the MVP-Munich GWAS datasets and the MVP-France datasets, meta-analyses were performed with the stratified disease subgroups FED and Barlow's disease. Fixed-effects models were applied, and heterogeneity was assessed using Cochran's Q test and I^2 statistics. Manhattan plots and Quantile-Quantile-plots were generated using R (version 4.2.2, 2022 The R Foundation for Statistical Computing) and ggplot2 package for visualization of GWAS results. Significant loci were reported with corresponding effect sizes, confidence intervals, and p-values.

4.6 Identification of Risk Loci

The independent signals were filtered by the clumping and thresholding method (LD r^2=0.2 1, *P1*=1e-5, *P2*=0.05, window=500kb) using PLINK 1.9, with 1000 Genomes Project Phase 3 used as the reference panel. Statistical analyses for the GWAS

ACCEPTED MANUSCRIPT

Downloaded from academic.oup.com/cardiovascres/advance-article/doi/10.1093/cvr/cvag263/9004318 by guest on 03 November 2026

are described in detail above. To correct for multiple testing, the standard Bonferroni testing threshold for genome-wide significance of $p<5x10^{-8}$ was applied. For $p<5x10^{-5}$, a significant correlation with MVP was suggestive. Risk loci ($p<5x10^{-8}$) and suggestive associations ($p<5x10^{-5}$) were further analyzed. Regional association plots were generated using LocusZoom. [63] For each lead SNP, the -$\log_{10}$ p-value of surrounding variants was plotted against their genomic coordinates. The genomic window size for plots was set to ±500 kb around the lead SNP. Any observed secondary signals were evaluated for independence using conditional analysis, where applicable. For each locus, a candidate gene was assigned based on linkage disequilibrium with the lead SNP and/or physical proximity to the associated region. Data base queries were performed to gather information on the candidate genes from phenome-wide association studies, expression in single-nucleus RNA sequencing data of heart tissue, mitral valve tissue, or fetal heart tissue, protein expression in mitral valve tissue, or gene expression in bulk RNA sequencing data of mitral valve tissue, respectively. (Tabula Sapiens was accessed on 15th January 2025 from https://registry.opendata.aws/tabula-sapiens; https://cvd.hugeamp.org/, https://tanglab.shinyapps.io/human_fetal_heart_scRNA/). [64–69]

4.7 Gene set enrichment analysis

Gene set enrichment analysis (GSEA) was performed to identify over-represented biological pathways and functions within the FED and Barlow's disease suggested candidate genes and genes nearest to candidate regions. The analysis utilized the enricher command from the ClusterProfiler R package (version 4.12.6). [70] The enrichment analysis was conducted against specific collections from the Molecular

ACCEPTED MANUSCRIPT

Downloaded from academic.oup.com/cardiovascres/advance-article/doi/10.1093/cvr/cvag263/9004318 by guest on 03 November 2026

Signatures Database (MSigDB) (version 2024.1.Hs). [71] Specifically, the following MSigDB gene set categories were used: H: Hallmark gene sets; C2: Curated gene sets; C5: GO gene sets. Statistical significance was determined via a one-sided hypergeometric test and statistically significant enriched terms ($p<0.01$) were selected for visualization.

4.8 Targeted variant-phenotype association analysis

To explore potential pleiotropic effects and contextualize the biological relevance of the identified variants, a targeted association analysis was performed in the UK Biobank across a predefined set of 30 cardiovascular phenotypes (application ID 25214). The selected phenotypes were chosen to capture different levels of MVP biology, including potential upstream predispositions (e.g., connective tissue disorders), downstream clinical consequences (e.g., atrial fibrillation), and broader cardiovascular traits. This exploratory approach was designed to assess whether the identified loci are specific to valvular disease or also associated with arrhythmic, structural, or systemic disease processes. These phenotypes were not treated as independent tests because of substantial clinical and biological overlap among traits; therefore, the analysis was interpreted as an exploratory assessment of pleiotropic associations. The ICD-10 codes of all 30 traits are listed in *Supplementary Table 2*.

Quality control considered individuals' missing rates <0.05 and kinship <0.124, variants' imputation info >0.4, and missing rate <0.02. Association analysis was performed for the identified variants and 30 risk traits using PLINK 1.9. To account for multiple testing,

ACCEPTED MANUSCRIPT

Downloaded from academic.oup.com/cardiovascres/advance-article/doi/10.1093/cvr/cvag263/9004318 by guest on 03 November 2026

Bonferroni correction was applied with significance set at $p<0.00833$. Associations were visualized using forest plots, highlighting key phenotypes linked to the genetic variants.

4.9 Single-nucleus RNA sequencing

Single-nucleus RNA sequencing (snRNA-seq) data from mitral valve tissue were analyzed. This dataset included 11,435 nuclei after quality control (before: 12,345) derived from two independent post-mortem mitral valve samples showing no macroscopic signs of cardiovascular or valve disease. The post-mortem interval ranged from two to three days. Nuclei isolation from mitral valve tissue was performed as described previously. [72] Sample preparation, processing of single nuclei, and sequencing is described in the *Supplementary Methods*. The two samples were processed and sequenced independently and were not pooled prior to sequencing. During downstream analysis, donor identity was retained and nuclei from both samples were integrated computationally. Downstream analysis was implemented using Seurat (version 5.2.1) [73] and data integration was performed using Harmony R package. [74] Principal component analysis (PCA) was used for dimension reduction and Uniform Manifold Approximation and Projection (UMAP) was used for data visualization. FindClusters command from Seurat was used to identify different clusters in the data and expression of canonical marker genes was used to annotate biologically relevant clusters.

4.10 Ethics statement

The local ethics review board of the Medical Faculty of the Technical University of Munich approved this study and the MVP-Munich cohort (5943/13, 247/16S and 352/21S). The investigation conformed to the principles outlined in the Declaration of Helsinki. The

ACCEPTED MANUSCRIPT

Downloaded from academic.oup.com/cardiovascres/advance-article/doi/10.1093/cvr/cvag263/9004318 by guest on 03 November 2026

other cohorts were approved by the respective local Institutional Review Boards of the participating institutions. [75,76] Written informed consent was obtained from the participants prior to the inclusion.

ACCEPTED MANUSCRIPT

Downloaded from academic.oup.com/cardiovascres/advance-article/doi/10.1093/cvr/cvag263/9004318 by guest on 03 November 2026

Acknowledgements, Funding

This work was supported by the following Institutes and Societies. The PROCAM-2 Study was initiated and conducted by the Leibniz Institute for Arteriosclerosis Research at the University of Münster under the leadership of G. Assmann. After his retirement, all data were transferred to the university for further scientific use. The later follow-up assessment was carried out with funds from the Institute of Epidemiology and Social Medicine, and DNA isolation was performed with financial support from the Dean of the medical faculty, both at the University of Münster. Genotyping was enabled through funds from the German Center for Cardiovascular Disease.

MVP-France was supported by the French Society of Cardiology and Leducq Foundation MITRAL Network of Excellence.

Martina Dreßen was supported by Förderverein Deutsches Herzzentrum.

We thank the KaBi-DHM for providing samples.

Conflicts of Interest

Markus Krane is a physician proctor and a member of the medical advisory board for Sanamedi, and has received speakers' honoraria from Edwards Lifesciences, AtriCure, Medtronic and Terumo.

Arnar Geirsson is a consultant for Edwards Lifescience and Medtronic.

All other authors have nothing to declare.

ACCEPTED MANUSCRIPT

Downloaded from academic.oup.com/cardiovascres/advance-article/doi/10.1093/cvr/cvag263/9004318 by guest on 03 November 2026

Data Availability Statement

The data underlying this article will be shared on reasonable request to the corresponding author.

ACCEPTED MANUSCRIPT

Downloaded from academic.oup.com/cardiovascres/advance-article/doi/10.1093/cvr/cvag263/9004318 by guest on 03 November 2026

References

1. Freed LA, Levy D, Levine RA, et al. Prevalence and Clinical Outcome of Mitral-Valve Prolapse. *New England Journal of Medicine*; 341. Epub ahead of print July 1999. DOI: 10.1056/NEJM199907013410101.

2. Levine RA, Hagége AA, Judge DP, et al. Mitral valve disease—morphology and mechanisms. *Nat Rev Cardiol* 2015; 12: 689–710.

3. Vahanian A, Beyersdorf F, Praz F, et al. 2021 ESC/EACTS Guidelines for the management of valvular heart disease: developed by the Task Force for the management of valvular heart disease of the European Society of Cardiology (ESC) and the European Association for Cardio-Thoracic Surgery (EACTS). *Eur Heart J* 2022; 43: 561–632.

4. Freed LA, Benjamin EJ, Levy D, et al. Mitral valve prolapse in the general population: the benign nature of echocardiographic features in the Framingham Heart Study. *J Am Coll Cardiol* 2002; 40: 1298–1304.

5. Le Tourneau T, Mérot J, Rimbert A, et al. Genetics of syndromic and non-syndromic mitral valve prolapse. *Heart* 2018; 104: 978–984.

6. Dina C, Bouatia-Naji N, Tucker N, et al. Genetic association analyses highlight biological pathways underlying mitral valve prolapsed. *Nat Genet* 2015; 47: 1206–1211.

7. Roselli C, Yu M, Nauffal V, et al. Genome-wide association study reveals novel genetic loci: A new polygenic risk score for mitral valve prolapse. *Eur Heart J* 2022; 43: 1668–1680.

8. Freed LA, Levy D, Levine RA, et al. Prevalence and clinical outcome of mitral-valve prolapse. *New England Journal of Medicine* 1999; 341: 1–7.

9. Toomer KA, Yu M, Fulmer D, et al. Primary cilia defects causing mitral valve prolapse. *Sci Transl Med* 2019; 11: eaax0290.

10. Anyanwu AC, Adams DH. Etiologic classification of degenerative mitral valve disease: Barlow's disease and fibroelastic deficiency. In: *Seminars in thoracic and cardiovascular surgery*. Elsevier, 2007, pp. 90–96.

ACCEPTED MANUSCRIPT

Downloaded from academic.oup.com/cardiovascres/advance-article/doi/10.1093/cvr/cvag263/9004318 by guest on 03 November 2026

11. van Wijngaarden AL, Kruithof BPT, Vinella T, et al. Characterization of degenerative mitral valve disease: differences between fibroelastic deficiency and Barlow's disease. *J Cardiovasc Dev Dis* 2021; 8: 23.

12. Herrera-Rivero M, Garvert L, Horn K, et al. A meta-analysis of genome-wide studies of resilience in the German population. *Mol Psychiatry* 2025; 30: 497–505.

13. Assmann G, Cullen P, Schulte H. Simple scoring scheme for calculating the risk of acute coronary events based on the 10-year follow-up of the prospective cardiovascular Munster (PROCAM) study. *Circulation* 2002; 105: 310–315.

14. Nishimura RA, Otto CM, Bonow RO, et al. 2014 AHA/ACC guideline for the management of patients with valvular heart disease: a report of the American College of Cardiology/American Heart Association Task Force on Practice Guidelines. *Circulation* 2014; 129: e521–e643.

15. Barlow JB, Bosman CK. Aneurysmal protrusion of the posterior leaflet of the mitral valve: an auscultatory-electrocardiographic syndrome. *Am Heart J* 1966; 71: 166–178.

16. Matsuura K, Kobayashi S, Konno K, et al. SIPA1L1/SPAR1 interacts with the neurabin family of proteins and is involved in GPCR signaling. *Journal of Neuroscience* 2022; 42: 2448–2473.

17. Brauch KM, Karst ML, Herron KJ, et al. Mutations in ribonucleic acid binding protein gene cause familial dilated cardiomyopathy. *J Am Coll Cardiol* 2009; 54: 930–941.

18. Lu D, Wang J, Li J, et al. Meox1 accelerates myocardial hypertrophic decompensation through Gata4. *Cardiovasc Res* 2018; 114: 300–311.

19. Mohamed JY, Faqeih E, Alsiddiky A, et al. Mutations in MEOX1, encoding mesenchyme homeobox 1, cause Klippel-Feil anomaly. *The American Journal of Human Genetics* 2013; 92: 157–161.

20. Moore KS, Moore R, Fulmer DB, et al. DCHS1, Lix1L, and the septin cytoskeleton: molecular and developmental etiology of mitral valve prolapse. *J Cardiovasc Dev Dis* 2022; 9: 62.

21. Durst R, Sauls K, Peal DS, et al. Mutations in DCHS1 cause mitral valve prolapse. *Nature* 2015; 525: 109–113.

22. Yada T, Sato T, Kaseyama H, et al. Chondroitin sulfate synthase-3: Molecular cloning and characterization. *Journal of Biological Chemistry* 2003; 278: 39711–39725.

ACCEPTED MANUSCRIPT

Downloaded from academic.oup.com/cardiovascres/advance-article/doi/10.1093/cvr/cvag263/9004318 by guest on 03 November 2026

23. O'Donnell A, Yutzey KE. Mechanisms of heart valve development and disease. *Development* 2020; 147: dev183020.

24. Grande-Allen KJ, Griffin BP, Calabro A, et al. Myxomatous mitral valve chordae. II: Selective elevation of glycosaminoglycan content. *J Heart Valve Dis* 2001; 10: 325–332.

25. Dainese L, Polvani G, Barili F, et al. Fine characterization of mitral valve glycosaminoglycans and their modification with degenerative disease.

26. Barber JE, Ratliff NB, Cosgrove 3rd DM, et al. Myxomatous mitral valve chordae. I: Mechanical properties. *J Heart Valve Dis* 2001; 10: 320–324.

27. Attardi LD, Reczek EE, Cosmas C, et al. PERP, an apoptosis-associated target of p53, is a novel member of the PMP-22/gas3 family. *Genes Dev* 2000; 14: 704–718.

28. Clemenceau A, Bérubé J, Bélanger P, et al. Deleterious variants in DCHS 1 are prevalent in sporadic cases of mitral valve prolapse. *Mol Genet Genomic Med* 2018; 6: 114–120.

29. Levine RA, Jerosch-Herold M, Hajjar RJ. Mitral valve prolapse: a disease of valve and ventricle. *Journal of the American College of Cardiology* 2018; 72: 835–837.

30. Jeanne M, Gould DB. Genotype-phenotype correlations in pathology caused by collagen type IV alpha 1 and 2 mutations. *Matrix Biology* 2017; 57: 29–44.

31. Burridge PW, Sharma A, Wu JC. Genetic and epigenetic regulation of human cardiac reprogramming and differentiation in regenerative medicine. *Annu Rev Genet* 2015; 49: 461–484.

32. Rivera-Feliciano J, Lee K-H, Kong SW, et al. Development of heart valves requires Gata4 expression in endothelial-derived cells.

33. Moskowitz IP, Wang J, Peterson MA, et al. Transcription factor genes Smad4 and Gata4 cooperatively regulate cardiac valve development. *Proceedings of the National Academy of Sciences* 2011; 108: 4006–4011.

34. Liu AC, Joag VR, Gotlieb AI. The emerging role of valve interstitial cell phenotypes in regulating heart valve pathobiology. *Am J Pathol* 2007; 171: 1407–1418.

35. Cai X, Zhang W, Hu J, et al. Tbx20 acts upstream of Wnt signaling to regulate endocardial cushion formation and valve remodeling during mouse cardiogenesis. *Development* 2013; 140: 3176–3187.

ACCEPTED MANUSCRIPT

Downloaded from academic.oup.com/cardiovascres/advance-article/doi/10.1093/cvr/cvag263/9004318 by guest on 03 November 2026

36. McMahon HT, Missler M, Li C, et al. Complexins: cytosolic proteins that regulate SNAP receptor function. *Cell* 1995; 83: 111–119.

37. Komatsu H, Kakehashi A, Nishiyama N, et al. Complexin-2 (CPLX2) as a potential prognostic biomarker in human lung high grade neuroendocrine tumors. *Cancer Biomarkers* 2013; 13: 171–180.

38. Li H, Zhao J, Zhong X, et al. CPLX2 regulates ferroptosis and apoptosis through NRF2 pathway in human hepatocellular carcinoma cells. *Appl Biochem Biotechnol* 2023; 195: 597–609.

39. Wang Z, Liu H, Gong Y, et al. Establishment and validation of an aging-related risk signature associated with prognosis and tumor immune microenvironment in breast cancer. *Eur J Med Res* 2022; 27: 317.

40. Feng P, Li Z, Li Y, et al. Characterization of different subtypes of immune cell infiltration in glioblastoma to aid immunotherapy. *Front Immunol* 2022; 13: 799509.

41. Jonsson G, Staaf J, Olsson E, et al. de JP, Oredsson S, Ringner M, Hoglund M, Borg A: High-resolution genomic profiles of breast cancer cell lines assessed by tiling BAC array comparative genomic hybridization. *Genes Chromosomes Cancer* 2007; 46: 543–558.

42. Chernova OB, Hunyadi A, Malaj E, et al. A novel member of the WD-repeat gene family, WDR11, maps to the 10q26 region and is disrupted by a chromosome translocation in human glioblastoma cells. *Oncogene* 2001; 20: 5378–5392.

43. Coon TA, Glasser JR, Mallampalli RK, et al. Novel E3 ligase component FBXL7 ubiquitinates and degrades Aurora A, causing mitotic arrest. *Cell cycle* 2012; 11: 721–729.

44. Liu Y, Lear T, Iannone O, et al. The proapoptotic F-box protein Fbxl7 regulates mitochondrial function by mediating the ubiquitylation and proteasomal degradation of survivin. *Journal of Biological Chemistry* 2015; 290: 11843–11852.

45. Liu C, Wang L, Chen W, et al. USP35 activated by miR let-7a inhibits cell proliferation and NF-κB activation through stabilization of ABIN-2. *Oncotarget* 2015; 6: 27891.

46. Park J, Kwon M-S, Kim EE, et al. USP35 regulates mitotic progression by modulating the stability of Aurora B. *Nat Commun* 2018; 9: 688.

47. Marzluff WF, Gongidi P, Woods KR, et al. The human and mouse replication-dependent histone genes. *Genomics* 2002; 80: 487–498.

ACCEPTED MANUSCRIPT

Downloaded from academic.oup.com/cardiovascres/advance-article/doi/10.1093/cvr/cvag263/9004318 by guest on 03 November 2026

48. Albig W, Kioschis P, Poustka A, et al. Human histone gene organization: nonregular arrangement within a large cluster. *Genomics* 1997; 40: 314–322.

49. Lowe BR, Maxham LA, Hamey JJ, et al. Histone H3 mutations: an updated view of their role in chromatin deregulation and cancer. *Cancers (Basel)* 2019; 11: 660.

50. Giancotti FG, Ruoslahti E. Integrin signaling. *Science (1979)* 1999; 285: 1028–1033.

51. Hynes RO. Integrins: bidirectional, allosteric signaling machines. *Cell* 2002; 110: 673–687.

52. Disatian S, Ehrhart Iii EJ, Zimmerman S, et al. Interstitial cells from dogs with naturally occurring myxomatous mitral valve disease undergo phenotype transformation. *Journal of Heart Valve Disease* 2008; 17: 402.

53. Geirsson A, Singh M, Ali R, et al. Modulation of transforming growth factor-β signaling and extracellular matrix production in myxomatous mitral valves by angiotensin II receptor blockers. *Circulation* 2012; 126: S189–S197.

54. Gao F, Chen Q, Mori M, et al. Integrin-mediated mTOR signaling drives TGF-β overactivity and myxomatous mitral valve degeneration in hypomorphic fibrillin-1 mice. *J Clin Invest*.

55. Vahanian A, Beyersdorf F, Praz F, et al. 2021 ESC/EACTS Guidelines for the management of valvular heart diseaseDeveloped by the Task Force for the management of valvular heart disease of the European Society of Cardiology (ESC) and the European Association for Cardio-Thoracic Surgery (EACTS). *European Journal of Cardio-Thoracic Surgery*.

56. Yu M, Kyryachenko S, Debette S, et al. Genome-Wide Association Meta-Analysis Supports Genes Involved in Valve and Cardiac Development to Associate With Mitral Valve Prolapse. *Circ Genom Precis Med* 2021; 14: E003148.

57. Group 3C Study. Vascular factors and risk of dementia: design of the Three-City Study and baseline characteristics of the study population. *Neuroepidemiology* 2003; 22: 316.

58. Delaneau O, Marchini J, Zagury J-F. A linear complexity phasing method for thousands of genomes. *Nat Methods* 2012; 9: 179–181.

59. Fairley S, Lowy-Gallego E, Perry E, et al. The International Genome Sample Resource (IGSR) collection of open human genomic variation resources. *Nucleic Acids Res* 2020; 48: D941–D947.

ACCEPTED MANUSCRIPT

Downloaded from academic.oup.com/cardiovascres/advance-article/doi/10.1093/cvr/cvag263/9004318 by guest on 03 November 2026

60. Marchini J, Howie B, Myers S, et al. A new multipoint method for genome-wide association studies by imputation of genotypes. *Nat Genet* 2007; 39: 906–913.

61. Purcell S, Neale B, Todd-Brown K, et al. PLINK: a tool set for whole-genome association and population-based linkage analyses. *The American journal of human genetics* 2007; 81: 559–575.

62. Purcell S. PLINK: a toolset for whole-genome association and population-based linkage analysis. *Am J hum genet* 2007; 81: 559–575.

63. Boughton AP, Welch RP, Flickinger M, et al. LocusZoom.js: interactive and embeddable visualization of genetic association study results. *Bioinformatics* 2021; 37: 3017–3018.

64. McLaren W, Gil L, Hunt SE, et al. The ensembl variant effect predictor. *Genome Biol* 2016; 17: 122.

65. Consortium* TTS, Jones RC, Karkanias J, et al. The Tabula Sapiens: A multiple-organ, single-cell transcriptomic atlas of humans. *Science (1979)* 2022; 376: eabl4896.

66. Jones RC, Karkanias J, Krasnow MA, et al. The Tabula Sapiens: A multiple-organ, single-cell transcriptomic atlas of humans. *Science (1979)* 2025; 376: eabl4896.

67. Absi TS, Galindo CL, Gumina RJ, et al. Altered ADAMTS5 expression and versican proteolysis: a possible molecular mechanism in barlow's disease. *Ann Thorac Surg* 2018; 105: 1144–1151.

68. Doll S, Dreßen M, Geyer PE, et al. Region and cell-type resolved quantitative proteomic map of the human heart. *Nat Commun* 2017; 8: 1469.

69. Cui Y, Zheng Y, Liu X, et al. Single-cell transcriptome analysis maps the developmental track of the human heart. *Cell Rep* 2019; 26: 1934–1950.

70. Wu T, Hu E, Xu S, et al. clusterProfiler 4.0: A universal enrichment tool for interpreting omics data. *The innovation*; 2.

71. Liberzon A, Birger C, Thorvaldsdóttir H, et al. The molecular signatures database hallmark gene set collection. *Cell Syst* 2015; 1: 417–425.

72. Lahm H, Jia M, Dreßen M, et al. Congenital heart disease risk loci identified by genome-wide association study in European patients. *Journal of Clinical Investigation*; 131. Epub ahead of print 19 January 2021. DOI: 10.1172/JCI141837.

73. Hao Y, Hao S, Andersen-Nissen E, et al. Integrated analysis of multimodal single-cell data. *Cell* 2021; 184: 3573–3587.

ACCEPTED MANUSCRIPT

Downloaded from academic.oup.com/cardiovascres/advance-article/doi/10.1093/cvr/cvag263/9004318 by guest on 03 November 2026

74. Korsunsky I, Millard N, Fan J, et al. Fast, sensitive and accurate integration of single-cell data with Harmony. *Nat Methods* 2019; 16: 1289–1296.

75. Dina C, Bouatia-Naji N, Tucker N, et al. Genetic association analyses highlight biological pathways underlying mitral valve prolapse. *Nat Genet* 2015; 47: 1206–1211.

76. Roselli C, Yu M, Nauffal V, et al. Genome-wide association study reveals novel genetic loci: a new polygenic risk score for mitral valve prolapse. *Eur Heart J* 2022; 43: 1668–1680.

ACCEPTED MANUSCRIPT

Downloaded from academic.oup.com/cardiovascres/advance-article/doi/10.1093/cvr/cvag263/9004318 by guest on 03 November 2026

Figures and Figure Legends

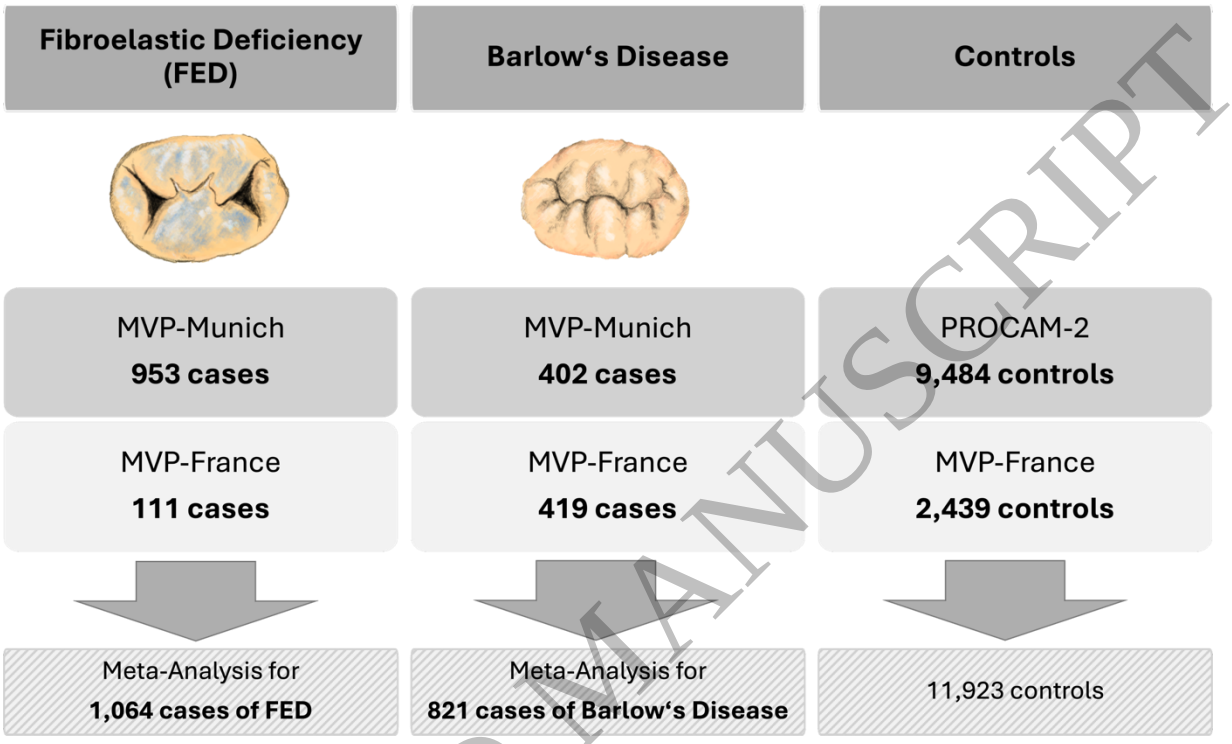


Fig. 1. Overview of patient cohorts included in GWAS meta-analysis for the mitral valve prolapse (MVP) subtypes of Fibroelastic deficiency (FED) and Barlow's disease. Patients from the German Heart Center constitute the MVP-Munich Cohort. Patients from the MVP-France study were included in the meta-analysis. Both cohorts were stratified into FED (n=1,064) and Barlow's disease (n=821) patients following intraoperative description and echocardiographic criteria. FED = Fibroelastic Deficiency, MVP = mitral valve prolapse, PROCAM-2: prospective cardiovascular Munster study.[12,13]

ACCEPTED MANUSCRIPT

Downloaded from academic.oup.com/cardiovascres/advance-article/doi/10.1093/cvr/cvag263/9004318 by guest on 03 November 2026

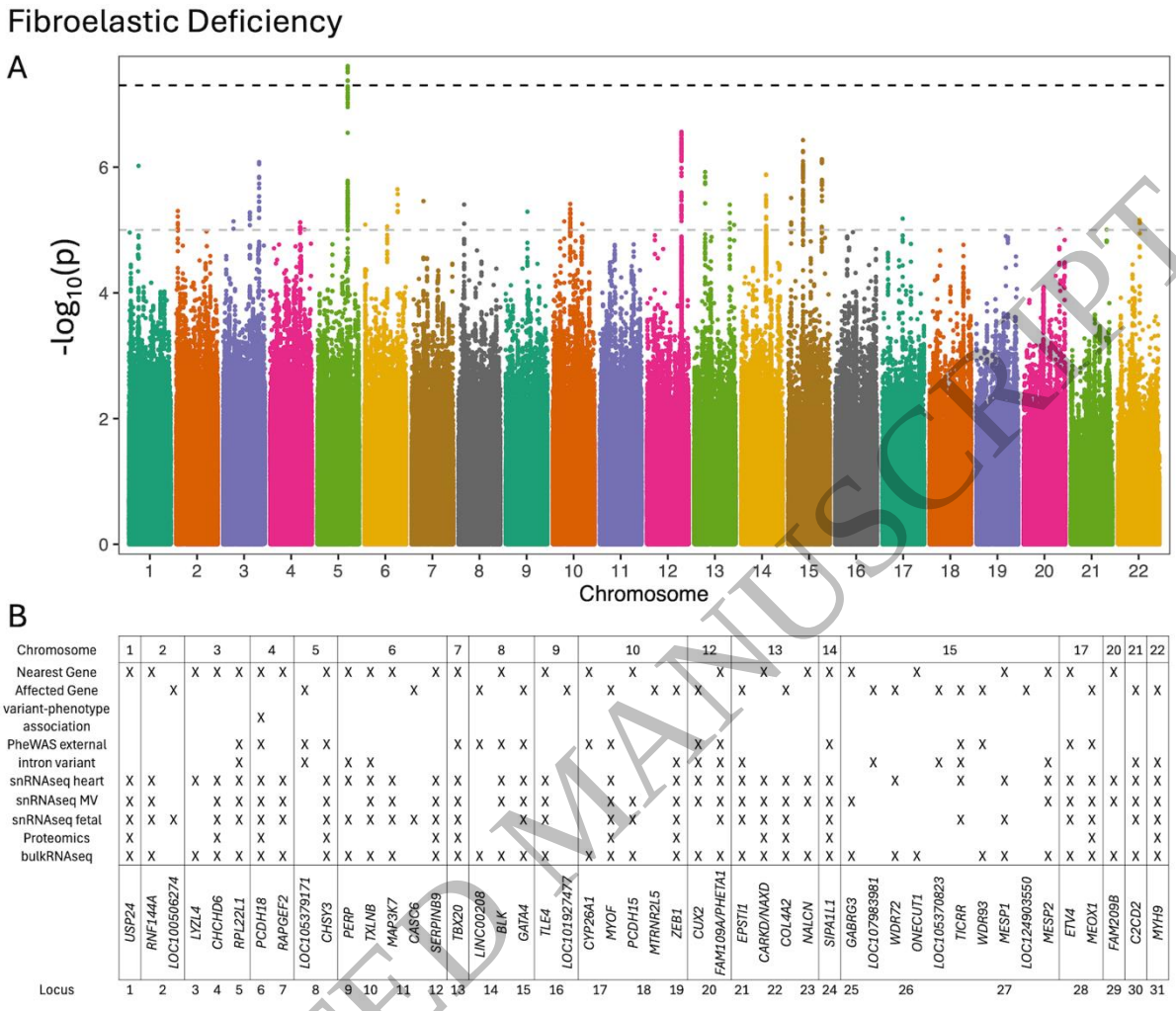


Fig. 2. Manhattan plot and genes at each locus of the Fibroelastic Deficiency (FED) meta-analysis. Meta-analysis included 1,064 FED patients. (A) Manhattan Plot representing the results of the meta-analysis for FED. The X axis shows the chromosomal positions; the Y axis shows the -log10(p)-values. The black dotted line indicates the genome-wide significant threshold ($p<5x10^{-8}$), and the grey dotted line indicates the sub-threshold cut-off of suggestive association ($p<5x10^{-5}$). (B) Annotated genes are shown for the respective genome-wide significant loci. The table below the Manhattan plot summarizes the available information for each associated locus. Gene annotation was based on proximity to the lead SNP and/or linkage disequilibrium with the associated region and does not imply causality.

ACCEPTED MANUSCRIPT

Downloaded from academic.oup.com/cardiovascres/advance-article/doi/10.1093/cvr/cvag263/9004318 by guest on 03 November 2026

The X indicates the availability of information for this gene in our targeted variant-phenotype association analysis, or in phenome-wide association studies, expression in single-nucleus RNA sequencing data of heart tissue, mitral valve tissue, or fetal heart tissue, protein expression in mitral valve tissue, or gene expression in bulk RNA sequencing data of mitral valve tissue, respectively. Intron variant: the sentinel variant is within the intron of the gene.

Fixed-effects models were applied, and heterogeneity was assessed using Cochran's Q test and I^2 statistics. Manhattan plots and Quantile-Quantile-plots were generated using R (version 4.2.2, 2022 The R Foundation for Statistical Computing) and ggplot2 package for visualization of GWAS results. Significant loci were reported with corresponding effect sizes, confidence intervals, and p-values. bulkRNAseq = bulk RNA sequencing, MV = mitral valve, PheWAS = phenome-wide association study, snRNAseq = single nucleus RNA sequencing.

ACCEPTED MANUSCRIPT

Downloaded from academic.oup.com/cardiovascres/advance-article/doi/10.1093/cvr/cvag263/9004318 by guest on 03 November 2026

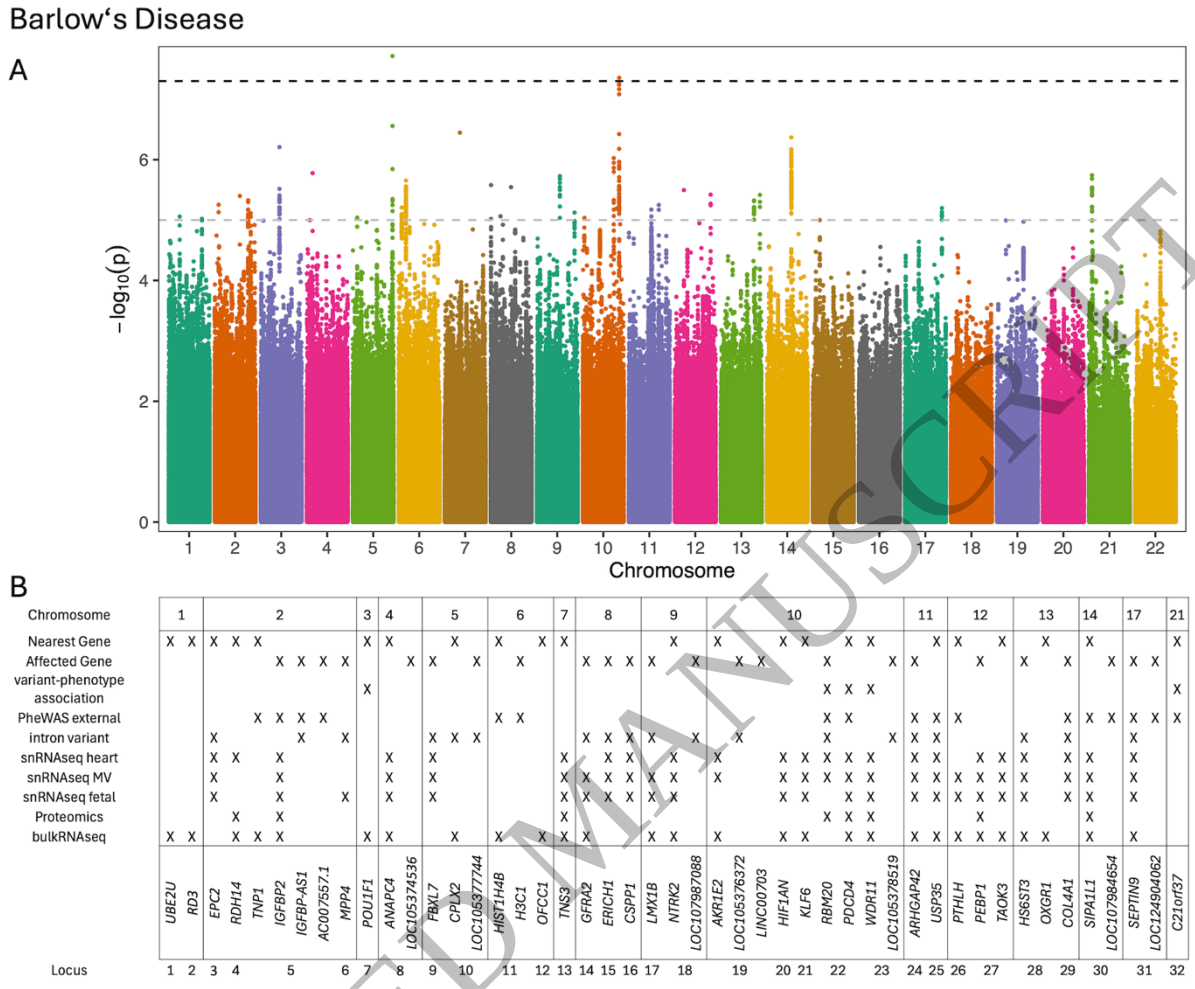


Fig. 3. Manhattan plot and genes at each locus of the Barlow's disease meta-analysis. Meta-analysis included 821 Barlow's disease patients. (A) Manhattan Plot representing the results of the GWAS meta-analysis for Barlow's disease. The X axis shows the chromosomal positions; the Y axis shows the -log10(p-values). The black dotted line indicates the genome-wide significant threshold ($p<5x10^{-8}$), and the grey dotted line indicates the sub-threshold cut-off of suggestive association ($p<5x10^{-5}$). (B) Annotated genes are shown for the respective genome-wide significant loci. The table below the Manhattan plot summarizes the available information for each associated locus. Gene

ACCEPTED MANUSCRIPT

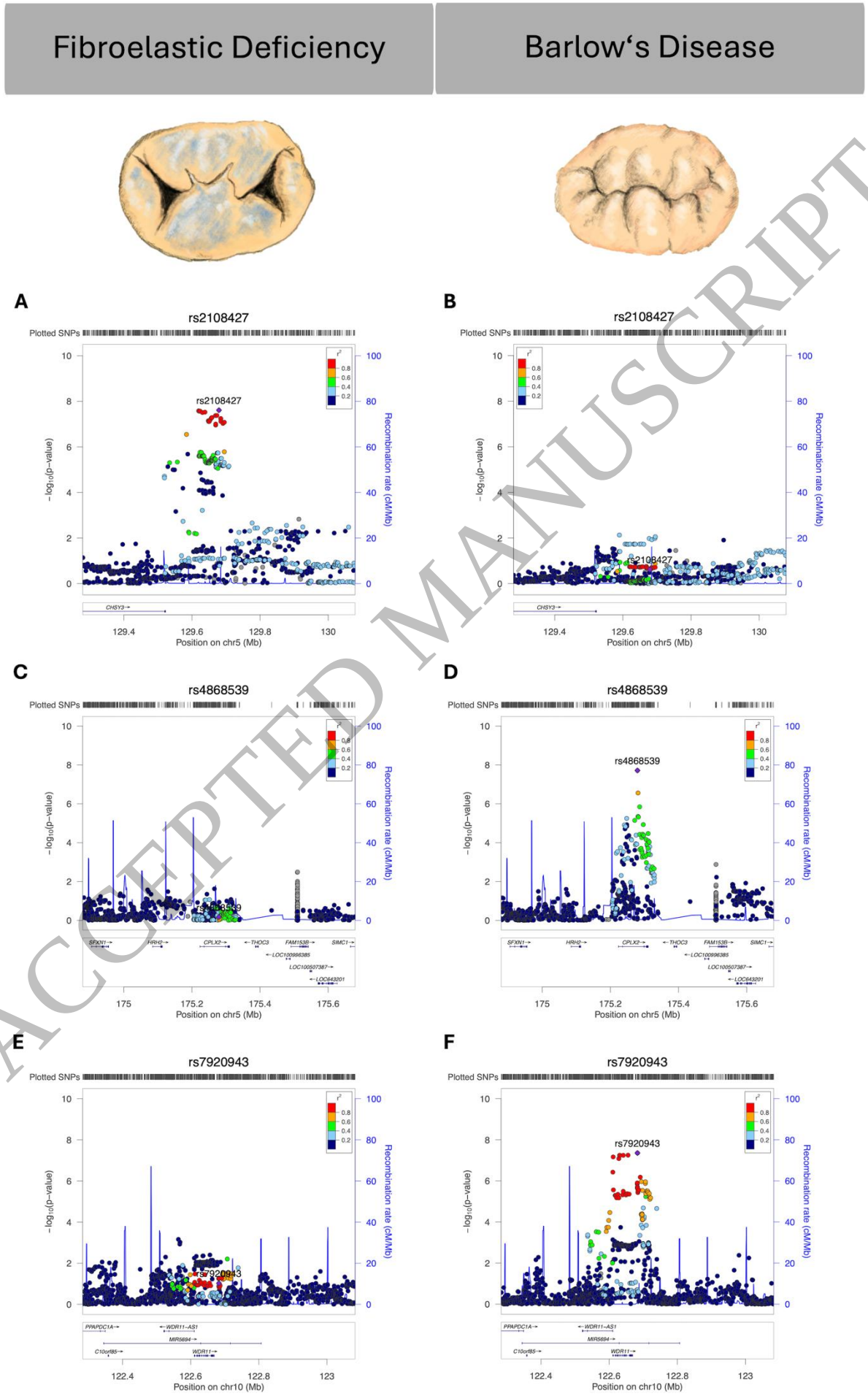
Downloaded from academic.oup.com/cardiovascres/advance-article/doi/10.1093/cvr/cvag263/9004318 by guest on 03 November 2026

annotation was based on proximity to the lead SNP and/or linkage disequilibrium with the associated region and does not imply causality. The X indicates the availability of information for this gene in our targeted variant-phenotype association analysis, or in phenome-wide association studies, expression in single-nucleus RNA sequencing data of heart tissue, mitral valve tissue, or fetal heart tissue, protein expression in mitral valve tissue, or gene expression in bulk RNA sequencing data of mitral valve tissue, respectively. Intron variant: the sentinel variant is within the intron of the gene.

Fixed-effects models were applied, and heterogeneity was assessed using Cochran's Q test and I^2 statistics. Manhattan plots and Quantile-Quantile-plots were generated using R (version 4.2.2, 2022 The R Foundation for Statistical Computing) and ggplot2 package for visualization of GWAS results. Significant loci were reported with corresponding effect sizes, confidence intervals, and p-values. bulkRNAseq = bulk RNA sequencing, MV = mitral valve, PheWAS = phenome-wide association study, snRNAseq = single nucleus RNA sequencing.

ACCEPTED MANUSCRIPT

Downloaded from academic.oup.com/cardiovascres/advance-article/doi/10.1093/cvr/cvag263/9004318 by guest on 03 November 2026



ACCEPTED MANUSCRIPT

Downloaded from academic.oup.com/cardiovascres/advance-article/doi/10.1093/cvr/cvag263/9004318 by guest on 03 November 2026

Fig. 4. Regional plots showing the linkage disequilibrium pattern for the identified genome-wide significant variants based on the European ancestry linkage disequilibrium observed from the 1000 Genomes Project. Meta-analyses included 1,064 FED and 821 Barlow's disease patients, respectively. On the left (A), the independent lead SNP in the risk locus for Fibroelastic Deficiency (rs2108427_T) is depicted. In comparison, the same region is depicted on the right (B) for the Barlow's disease GWAS meta-analysis, where no independent locus with genome-wide significant association was found in this region. Below, the independent lead SNPs in the risk loci with genome-wide association with Barlow's disease are depicted. The risk locus rs4868539_A has no signal in FED (C) but shows significance in the Barlow's disease subgroup (D). The risk locus rs7920943_A has no significant association with FED (E) but is significant in the Barlow's disease subgroup (F).

The independent signals were filtered by the clumping and thresholding method (LD r2=0.2 1, P1=1e-5, P2=0.05, window=500kb) using PLINK 1.9, with 1000 Genomes Project Phase 3 used as the reference panel. To correct for multiple testing, the standard Bonferroni testing threshold for genome-wide significance of $p<5x10\text{-}8$ was applied. For $p<5x10\text{-}5$, a significant correlation with MVP was suggestive. Risk loci ($p<5x10\text{-}8$) and suggestive associations ($p<5x10-5$) were further analyzed.

ACCEPTED MANUSCRIPT

Downloaded from academic.oup.com/cardiovascres/advance-article/doi/10.1093/cvr/cvag263/9004318 by guest on 03 November 2026

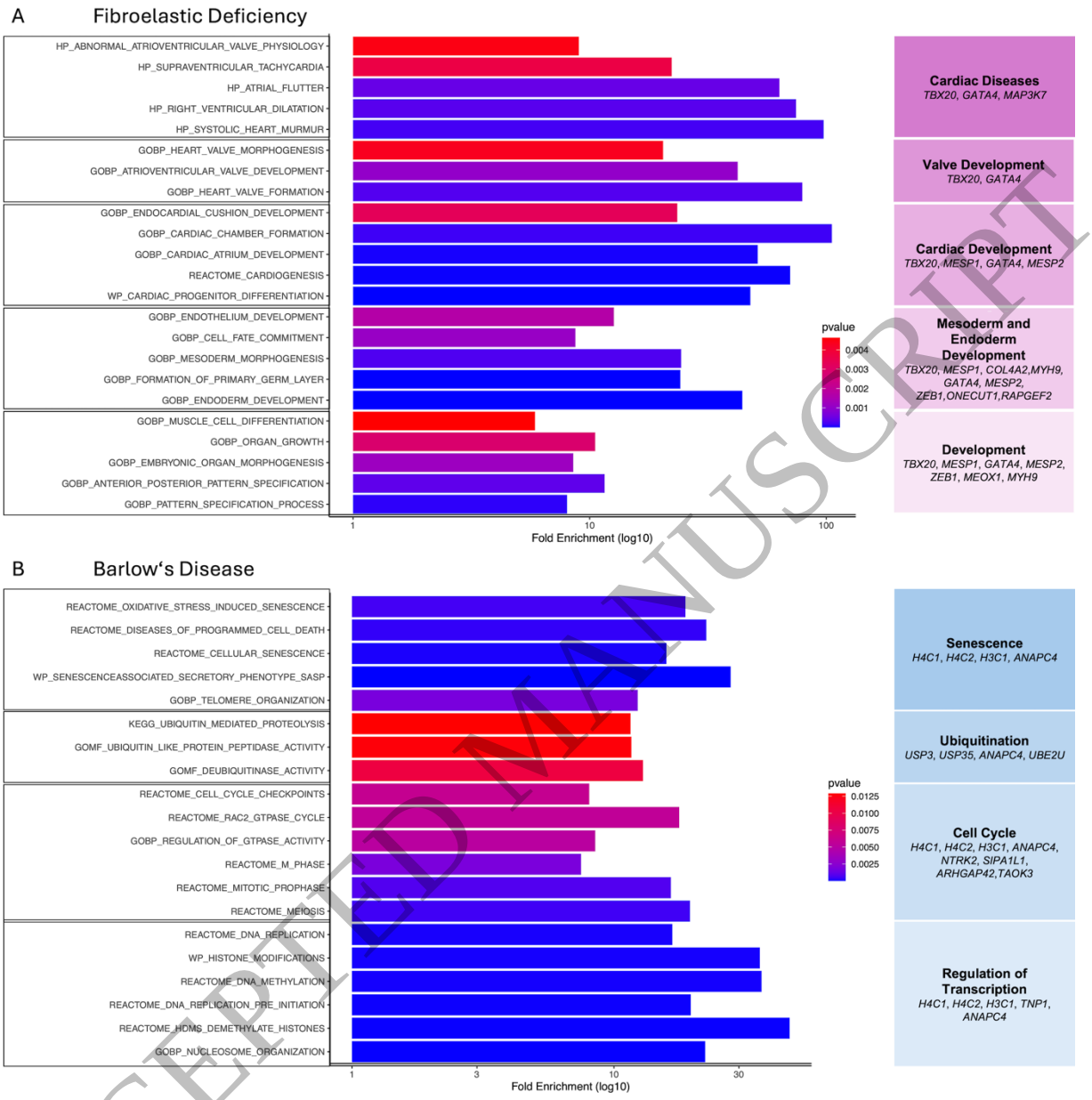


Fig. 5. Fold enrichment from gene set enrichment analysis of significantly enriched Gene Ontology Biological Process (GOBP) categories for FED (A) and Barlow's disease (B). Bar plots show the fold enrichment of selected GOBP categories based on gene set enrichment analysis. Only categories with FDR-adjusted p-values (p.adjust) <0.05 are shown. The x-axis represents fold enrichment, while the y-axis lists the enriched GOBP terms. Bar length indicates the magnitude of enrichment, and bars are colored by $-\log_{10}$(p.adjust) to reflect

ACCEPTED MANUSCRIPT

Downloaded from academic.oup.com/cardiovascres/advance-article/doi/10.1093/cvr/cvag263/9004318 by guest on 03 November 2026

statistical significance. Enrichment was calculated relative to a background of all protein-coding genes tested. These results highlight overrepresentation of genes involved in the development of FED and Barlow's disease.

The analysis utilized the enricher command from the ClusterProfiler R package (version 4.12.6). [70] The enrichment analysis was conducted against specific collections from the Molecular Signatures Database (MSigDB) (version 2024.1.Hs). [71] Specifically, the following MSigDB gene set categories were used: H: Hallmark gene sets; C2: Curated gene sets; C5: GO gene sets. Statistical significance was determined via a one-sided hypergeometric test and statistically significant enriched terms ($p<0.01$) were selected for visualization.

ACCEPTED MANUSCRIPT

Downloaded from academic.oup.com/cardiovascres/advance-article/doi/10.1093/cvr/cvag263/9004318 by guest on 03 November 2026

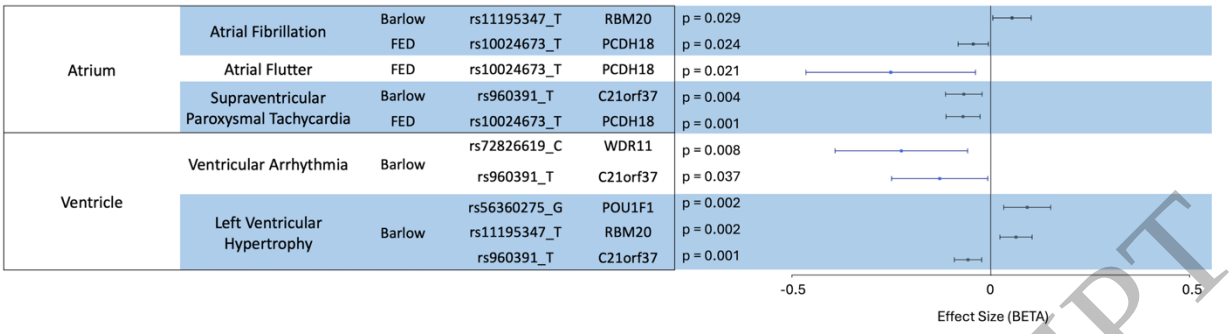


Fig. 6. Forest Plot showing the targeted variant-phenotype association analysis of cardiac diseases with a suggested association with Fibroelastic Deficiency (FED) or Barlow's disease. The effective alleles specified are the risk-increasing alleles for FED and Barlow's disease.

A targeted association analysis was performed across 30 MVP-related traits using the UK Biobank dataset (application ID 25214). Information for 30 MVP-related traits were retrieved, including atrial fibrillation, atrial flutter, paroxysmal supraventricular tachycardia, left ventricular hypertrophy, and ventricular arrhythmia. The ICD-10 codes of all 30 traits are listed in *Supplementary Table 2*. Quality control considered individuals' missing rates <0.05 and kinship <0.124, variants' imputation info >0.4, and missing rate <0.02. Association analysis was performed for the identified variants and 30 risk traits using PLINK 1.9. To account for multiple testing, Bonferroni correction was applied with significance set at $p<0.00833$. Associations were visualized using forest plots, highlighting key phenotypes linked to the genetic variants.

ACCEPTED MANUSCRIPT

Downloaded from academic.oup.com/cardiovascres/advance-article/doi/10.1093/cvr/cvag263/9004318 by guest on 03 November 2026

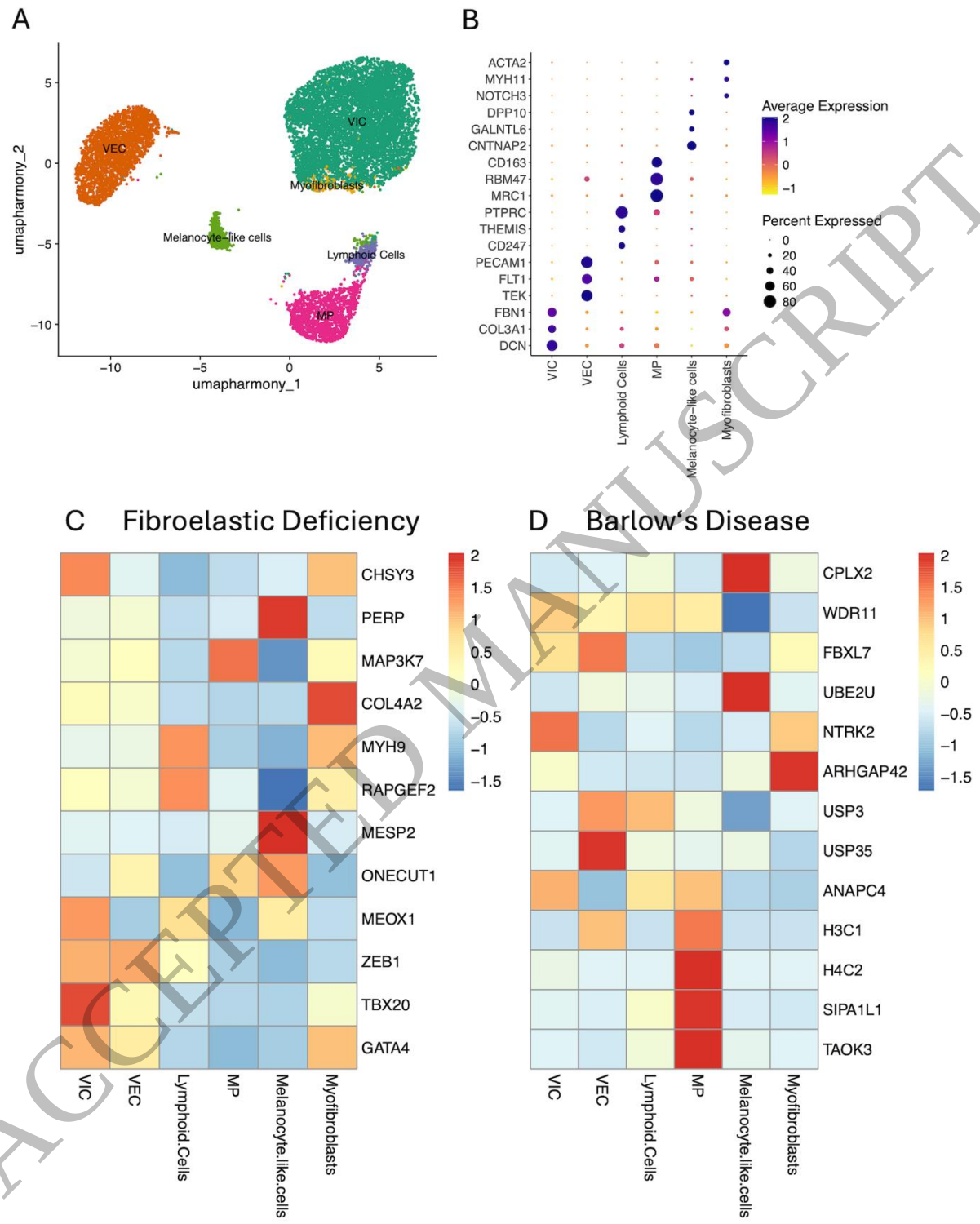


Fig. 7. Single-Nucleus RNA-Sequencing of Mitral Valve Tissue. This dataset included 11,435 nuclei after quality control (before: 12,345) from two post-mortem mitral valve samples showing

ACCEPTED MANUSCRIPT

Downloaded from academic.oup.com/cardiovascres/advance-article/doi/10.1093/cvr/cvag263/9004318 by guest on 03 November 2026

no macroscopic signs of cardiovascular or valve disease. (A) Uniform Manifold Approximation and Projection (UMAP) plot of single-nucleus RNA sequencing data revealed six cell clusters in mitral valve tissue. (B) Dot-plot visualizing the expression of canonical marker genes in associated cell types. (C, D) Heat-map showing the cell-type specific expression of suggested candidate genes and genes nearest to candidate regions in Fibroelastic Deficiency (C) or Barlow's disease (D), respectively. Highly expressed genes are colored in red, low expression is colored in blue. EC = endothelial cells, FED = Fibroelastic Deficiency, MPs = macrophages, UMAP = Uniform Manifold Approximation and Projection, VECs = valvular endothelial cells, VICs = valvular interstitial cells.

Tables

Table 1: Genome-wide associated risk loci of the meta-analysis for FED or Barlow's disease. Genomic build GRCh37 was used. Chr = chromosome, *CHSY3* = Chondroitin Sulfate Synthase 3, *CPLX2* = Complexin 2, I^2 = percentage of total variation attributable to between-study heterogeneity, MAF = minor allele frequency, NRA = non-risk allele, OR = Odd's Ratio, P = p-value, Pos (bp) = position (base pair), Q = Cochran's Q test, RA = risk allele, SE = standard error, *WDR11* = WD Repeat Domain 11.

Risk Locus for Fibroelastic Deficiency										
rsID	Chr	pos (bp)	Locus	RA	NRA	MAF	OR	P	Q	I^2
rs2108427	5	129679124	*CHSY3*	T	G	0.458	1.306	2.46×10^{-08}	0.1215	58.30

ACCEPTED MANUSCRIPT

Downloaded from academic.oup.com/cardiovascres/advance-article/doi/10.1093/cvr/cvag263/9004318 by guest on 03 November 2026

Risk Loci for Barlow's Disease										
rsID	Chr	pos (bp)	Locus	RA	NRA	MAF	OR	P		
rs4868539	5	175279441	*CPLX2*	A	G	0.465	1.335	$1.93x10^{-08}$	0.9688	0.00
rs7920943	10	122682968	*WDR11*	A	G	0.232	1.501	$4.42x10^{-08}$	0.1656	47.97

Linear regression was applied for continuous traits, while logistic regression was used for binary traits, with covariates including age, sex, and principal components (the first ten to account for population stratification). To adjust for population stratification, multidimensional scaling was performed in PLINK. [62]. Fixed-effects models were applied, and heterogeneity was assessed using Cochran's Q test and I^2 statistics. To correct for multiple testing, the standard Bonferroni testing threshold for genome-wide significance of p<5x10-8 was applied.

ACCEPTED MANUSCRIPT

Downloaded from academic.oup.com/cardiovascres/advance-article/doi/10.1093/cvr/cvag263/9004318 by guest on 03 November 2026